Environmental Research 218 (2023) 114984

Contents lists available at ScienceDirect

Environmental Research

journal homepage: www.elsevier.com/locate/envres

Porous nanocomposites for sorptive elimination of ibuprofen from synthetic wastewater and its molecular docking studies

M. Rajamehala [a,*], A. Muthu Kumara Pandian [a], M. Rajasimman [b], B. Gopalakrishnan [b]

[a] Department of Biotechnology, Vivekanandha College of Engineering for Women, Tiruchengode, Namakkal, 637205, Tamilnadu, India
[b] Department of Chemical Engineering, Annamalai University, Annamalai Nagar, 608002, India

ARTICLE INFO

Keywords:
Pharmaceuticals
Nanocomposite
Contaminants
Moringa olifera, isotherm
Kinetics

ABSTRACT

Pharmaceuticals are a new developing pollutant that is threatening aquatic ecosystems and impacting numerous species in the ecosystem. The aim of this study is the green synthesis of TiO_2–Fe_2O_3-Chitosan nanocomposites in conjunction with *Moringa olifera* leaves extract and its applicability for ibuprofen removal. Various characterization studies were performed for the synthesized nanocomposites. Box-Behnken design (BBD) is employed to optimize pH, agitation speed, and composite dosage. Equilibrium results show that adsorption process matches with Langmuir isotherm, demonstrating adsorption on the nanocomposite's homogenous surface and follows pseudo-first-order kinetics. Using the BBD, pH, adsorbent dose, and agitation speed were examined as adsorption parameters. Ibuprofen elimination was demonstrated to be most successful at a pH of 7.3, using 0.05 g of nanocomposites at a rotational speed of 200 rpm. Thermodynamic parameters for ibuprofen sorption were carried out and the ΔH and ΔS was found to be 76.23 & 0.233. Molecular Docking was performed to find the interaction between the pollutant and the nanocomposite. UV–vis spectra confirm the 243 nm absorption band corresponding to the nanocomposite's surface plasmon resonances. Fourier transform infrared spectroscopy spectra relate this band to a group of nanocomposites. The findings of this work emphasize the importance of TiO_2–Fe_2O_3-Chitosan nanocomposites for removing ibuprofen from wastewater.

1. Introduction

India is a big country that ranks fifth in the world's pharmaceutical markets and third in terms of the number of drugs it sells. The pharmaceutical industry makes a bigger difference to the world economy than some of the other health care industries. With the continual advances in technologies, there is an increased demand for the pharmaceutical products (Fröhlich et al., 2019). It was found that pharmaceuticals with both active ingredients and excipients have an effect on the environment and, in turn, on public health (Streit et al., 2021). Pharmaceutical companies generate a massive amount of waste, regardless of their size or scale of operation. Pharmaceutical waste can come from a variety of sources, the most prevalent of which are hospital waste disposal items, agricultural waste from veterinary use, trash from livestock feed additives, and waste from manufacturing companies. These wastes were allowed to be released into the environment, which led to the accumulation of poisonous compounds in drinking water, surface water, wastewater, ground water, and sewage, all of which are hazardous to the health of humans. It was discovered that pharmaceuticals or wastes from pharmaceuticals were released into the environment mostly as a result of incorrect disposal or usage. (Thomas, 2017). It has been found that their presence in the environment, water bodies and sewage, can have an effect on the health of both humans and aquatic life (Heberer, 2002). Amongst the various non-steroidal anti--inflammatory pharmaceutical drugs, frequently detected compounds in aquatic system are ibuprofen, ketoprofen, paracetamol, amoxillin (Ahmed, 2017).

Ibuprofen (IBU) is one of the most commonly used medicines in the world. It's often used to treat migraines, fevers, muscle pain, and toothaches. The annual production is expected to be 13,500 tonnes (Gilevska et al., 2015) and several hundred tonnes is consumed by developing countries (Rainsford, 2012) discarded in domestic litter without proper disposal. Only about 15–23 percent of ingested Ibuprofen is absorbed, with the remainder excreted in the urine and approximately 24.6 μg/L concentration has been found in water (Rainsford, 2012).

Emerging pollutants from water streams and aquatic systems are a challenge for researchers worldwide and many technological solutions

* Corresponding author.
E-mail address: rajamehala@gmail.com (M. Rajamehala).

https://doi.org/10.1016/j.envres.2022.114984
Received 29 September 2022; Received in revised form 15 November 2022; Accepted 29 November 2022
Available online 1 December 2022
0013-9351/© 2022 Elsevier Inc. All rights reserved.

to eliminate dangerous pharmaceutical compounds have been developed (Tiwari et al., 2017). The disadvantages of the traditional methods employed for the elimination of pollutant are: reduced efficiency and greater prices, production of undesirable toxic by-products or metabolites as a consequence of chemical reactions, extreme use of potentially dangerous substances, complex and costly as well as cumbersome operation, limited capacity to tarnish numerous different contaminants, poor efficacy in removing vast numbers of compounds, and the inability to reduce contamination (Rasheed et al., 2019; Kamal et al., 2015; Mohmood et al., 2013).

Adsorption is a promising, eco-friendly and cost-effective approach to waste water pollutant because it is flexible in nature and easy to operate (Mitra et al., 2017). Metallic nanoparticles can be identified by their specific physical and chemical features, which include a high surface area, a tiny size, and a morphology (Dragoi and Vasseghian, 2021; Vasseghian et al., 2022a,b; Liu et al., 2022). These nanoparticles have been investigated for their potential use in water treatment. (Aguilar-Pérez et al., 2021). Zero-valent metal nanoparticles, metal oxide nanoparticles, carbon nanotubes, and nanocomposites are the most studied nano-adsorbents for water treatment (Aguilar-Pérez et al., 2021; Rasheed et al., 2020). Titanium dioxide, often known as TiO_2, is one of the nanoparticles that has received the most attention from researchers due to its cost-effectiveness, chemical inertness, commercial availability, non-toxicity, and eco-friendliness. Because of the high band gap of 3.2 eV that it possesses, pure TiO_2 can only absorb light in the ultraviolet portion of the spectrum. To reduce the band gap, a number of research were carried out, and as a result, the TiO_2 particles can now be triggered by visible light (Leong et al., 2014). Chitosan is the second most widely biopolymer, with nontoxic, antimicrobial, bioactive, and biodegradable properties (Wu et al., 2022). Chitosan has been extensively researched for its use in wastewater treatment as good biosorbent, chelating agents, and upholds other nano-sized materials. It is primarily extracted as chitin from crustacean waste, squid, and oysters**.** Chitosan can also be utilized as an adsorbent in the treatment of water with various functional groups, such as amino and hydroxyl groups. (Ahmad et al., 2020; Zhang et al., 2022; Yasser and Elena, 2018). Because of its biocompatibility, biodegradability, nontoxicity, and adsorption properties, chitosan is the most commonly used polymer in the preparation of nanocomposite materials. These characteristics are commonly used to modify different metal nanoparticles (Mahmoudi et al., 2009; Xia et al., 2022). There are literatures available on ibuprofen removal by sorption using sorbents like Quercus Brantii *(*Nourmoradi et al., 2018), physically and chemically treated date stone biochar (Chakraborty et al., 2020), iron nanocomposite (Ali et al., 2016), polystyrene, ultra-high molecular weight polyethylene, average molecular weight medium density polyethylene, and polypropylene (Velazquez, 2020). Show et al. (2021) performed a review on sorptive removal of ibuprofen. But still, there is a desire among the researchers and scientists across the globe to find sorbents to remove the pollutants with more efficiency.

So far, no study is available on the use of TiO_2/Fe_2O_3/Chitosan nanocomposites for the sorptive removal of ibuprofen and its molecular docking analysis. So, the current study deals with the synthesis of TiO_2/Fe_2O_3/Chitosan nanocomposites using *Moringa olifera* leaf extracts and different analytical methods were used to characterize the nanocomposite. The batch adsorption behavior of the materials was studied by adjusting various factors. The adsorption isotherms, kinetics, and thermodynamics were also investigated along with the nanocomposite's stability and its capacity for recycling.

2. Materials and methods

All the reagents and chemicals used for this research work were of analytical reagent (AR) grade and purchased from Hi-Media laboratories, Chennai, India. De-ionized double distilled water is used throughout the study. UV–Visible Spectrophotometer (Shimadzu UV-1700 spectrophotometer, India) is used for the estimation of concentrations in the samples. Ibuprofen stock solition is prepared by dissolving 1 g of ibuprofen tablet powder in 1000 mL of water. From the stock solution, other concentrationsof ibuprofen were prepared.

2.1. Preparation of Moringa olifera leaf extract

After collecting the *Moringa olifera* leaves, they were washed three times with double-distilled water and then allowed to air dry at room temperature for two days. Using a blender, the dried leaves were ground into a powder. After dissolving 10 g of leaf powder in 100 mL of double-distilled water, the mixture is heated to 50 °C for 2 h. After being filtered via Whatmann filter paper, the extract is then chilled to 4 °C in preparation for future usage (Rajamehala et al., 2022).

2.2. Synthesis of TiO_2 nanoparticles

10 mL of 0.3 M Titanium Tetra Isopropoxide is added dropwise to 50 mL of leaf extract. The solution is continuously stirred until color changes from light yellow to brownish yellow. Later the brownish yellow color precipitate is collected and dried at 60 °C for 2 h in hot air oven. Mortar and pestle are used to grind the dried precipitate into a fine powder. The obtained nanoparticle will be kept for use in subsequent experiments (Balaji et al., 2019).

2.3. Synthesis of iron oxide nanoparticles

Ferric chloride is used as a precursor for iron oxide nanoparticle synthesis. The above obtained filtrate is mixed with 0.1 M Ferric chloride in 1:1 ratio and vigorously stirred using a magnetic stirrer. Formation of black color indicates the synthesis of iron oxide nanoparticles (Bhuiyan et al., 2020).

2.4. Preparation of TiO_2–Fe_2O_3-Chitosan nanocomposite

2 g of Chitosan is dissolved in 100 mL of 2% glacial acetic acid. The mixture is stirred for 30 min using mechanical stirrer and then sonicated for 1 h using ultrasonicator. Add 1.53 g of synthesized iron oxide nanoparticle and 0.2 g of TiO_2 nanoparticle and stir vigorously for 1.5 h and then homogenise the solution using sonicator for 2 h pH is maintained at 4.5 using 0.1 M NaOH and HCl. The obtained solution is centrifuged and the pellet is dried in hot air oven for 5 h at 80 °C.The dried powder is grinded using mortar and pestle and used for further studies. (Bhanvase et al., 2019). The obtained nanocomposite was characterized using SEM, EDAX, XRD, FTIR, and XPS.

2.5. Experimental method for sorption

BBD is utilized for the purpose of optimizing the parameters involved in the ibuprofen removal process. These factors include pH, agitation speed, and sorbent dosage. Experiments were performed in 250 mL Erlenmeyer flask. Ibuprofen solution with a concentration of 50 ppm is drawn up to a volume of 100 mL. Adjustments are made to the pH, the rate of agitation, and the amount of sorbent used for each run. After it has been allowed to incubate for 1 h 30 min, the solution is filtered through whatmann filter paper. After collecting the adsorbed sorbent, a UV–Visible Spectrophotometer set to 243 nm is used to determine the amount of ibuprofen that was found in the filtrate.

The Removal Percentage of Ibuprofen is given by

$$\% = \frac{C_o - C_e}{C_o} \times 10 \quad (1)$$

Adsorption capacity (q_e) is calculated by

$$q_e = \frac{(C_o - C_e)V}{m} \quad (2)$$

Table 1
Isotherm used for sorption of Ibuprofen.

Isotherm	Linear form	Reference
Langmuir	$\frac{1}{q_e} = \frac{1}{q_m} + \frac{1}{q_m b C_e}$	Langmuir (1916)
Freundlich	$\log q_{e=} \log K_f + \frac{1}{n} \log C_e$	Freundlich (1906)
Dubinin-Radushkevich	$\ln q_{e=} \ln q_s - k_{ad} \in^2$	Dubinin (1960)
Temkin	$q_{e=} \frac{RT}{b_T} \ln A_T + \frac{RT}{b_T} \ln C_e$	Temkin and Pyzhev (1940)

Table 2
Operating variable range and values for ibuprofen removal.

Variables	Code	Levels		
		−1	0	1
pH	A	5	7	9
Agitation Speed, (rpm)	B	100	150	200
Sorbent Dosage (g/l)	C	0.01	0.05	0.09

Table 3
BBD and ibuprofen removal using TiO_2/Fe_2O_3/chitosan nanocomposite.

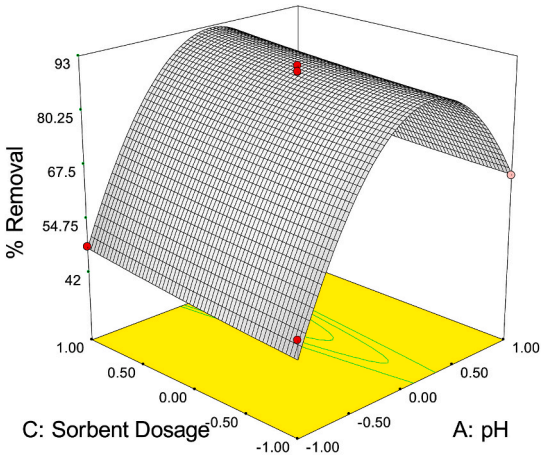
Std. Order	Run order	A	B	C	Ibuprofen removal, %	
					Experimental	Theoretical
12	1	1	0	0	95.210	93.042
14	2	1	−1	−1	89.420	89.353
7	3	1	−1	1	48.210	47.013
4	4	1	0	0	69.830	67.695
15	5	1	−1	0	87.830	89.353
1	6	1	0	−1	42.300	44.435
3	7	1	1	0	43.120	45.585
13	8	1	1	0	90.810	89.353
5	9	1	0	−1	47.140	42.838
9	10	1	1	−1	85.420	87.587
8	11	1	0	1	64.230	68.532
6	12	1	0	0	65.420	65.718
11	13	1	−1	−1	92.340	90.502
2	14	1	−1	1	68.290	65.825
10	15	1	0	0	86.230	88.067

Table 4
Results of the ANOVA about the removal of Ibuprofen.

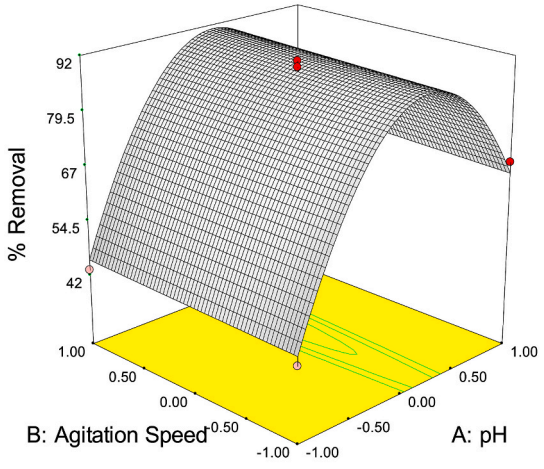
Source	Sum of Squares	df	Mean Square	F-value	P-value
Model	5184.90	9	576.10	36.43	0.0005
A	946.12	1	946.12	59.830	0.0006
B	4.56	1	4.56	0.290	0.6143
C	31.13	1	31.13	1.970	0.2196
AB	0.13	1	0.13	0.008	0.9314
AC	1.28	1	1.28	0.081	0.7877
BC	1.06	1	1.06	0.067	0.8059
A^2	4145.96	1	4145.96	262.190	*< 0.0001*
B^2	0.01	1	0.01	0.000	0.9850
C^2	0.61	1	0.61	0.038	0.8522
Residual	79.06	5	15.81		
Lack of Fit	74.62	3	24.87	11.190	0.0832
Pure Error	4.45	2	2.22		
Cor Total	5263.96	14			

Std. Dev- 3.98; R-Squared-0.9850; Mean - 71.72; Adj R-Squared-0.9579; C.V. %-5.54; Pred R-Squared- 0.7713; PRESS- 1203.89; Adeq Precision- 15.463.

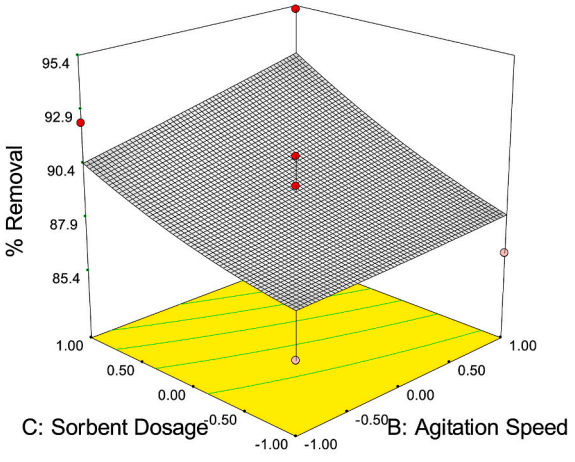
Where C_o and C_e – Ibuprofen concentration at initial and final (mg/L), q_e - adsorption capacity (mg/g),V - Volume of solution (mL), m - mass of sorbent (g) (Jayakumar et al., 2021).



(a)



(b)



(c)

Fig. 1. Interactive effect of variables on Ibuprofen removal (a) pH & Sorbent Dosage (b)pH & Agitation Speed (c) Sorbent Dosage & Agitation Speed.

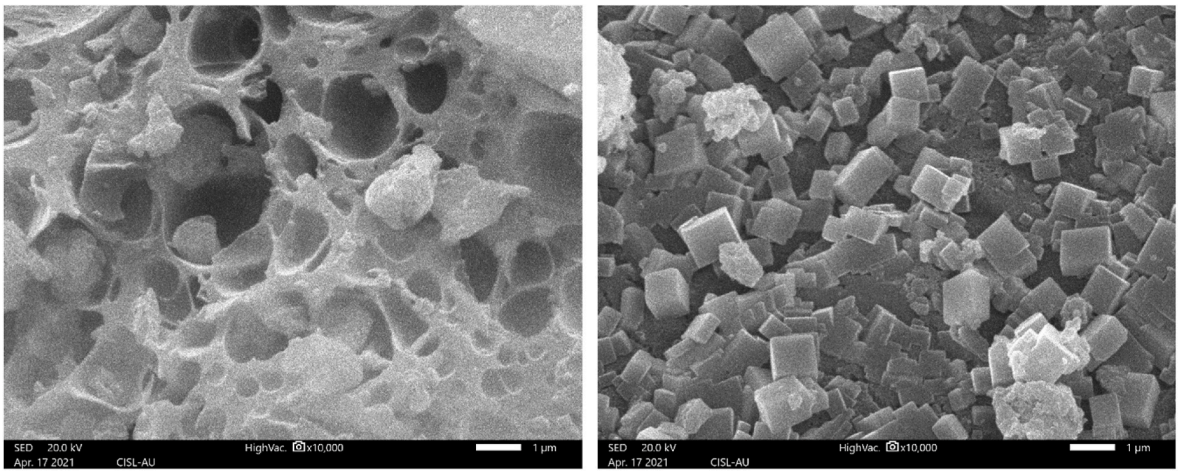


Fig. 2. SEM images of synthesized nanocomposite.

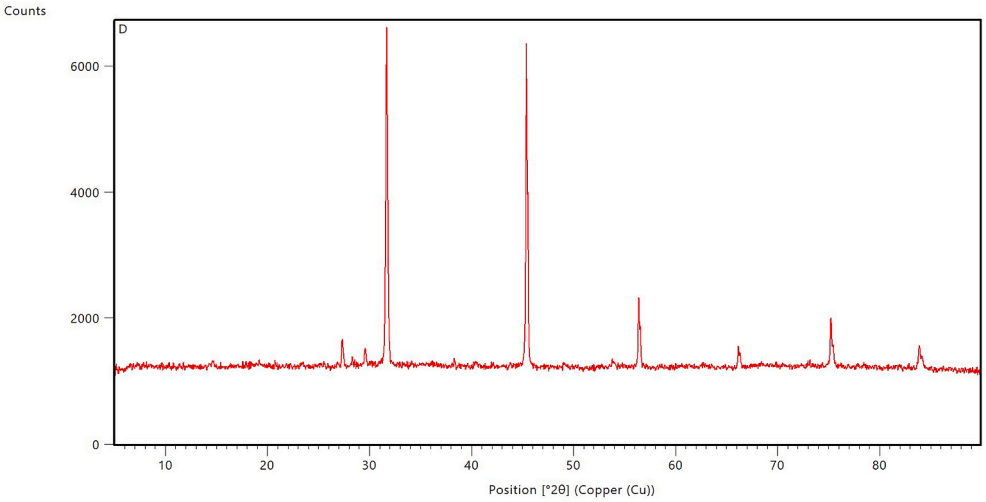


Fig. 3. XRD spectra of synthesized nanocomposite after sorption.

Table 5
FTIR of nanocomposite before and after sorption of Ibuprofen.

Wavelength Range (cm^{-1})	TiO_2/Fe_2O_3/Chitosan Nanocomposite		Functional Groups
	Before Sorption	After Sorption	
3500–3000	3312.047 3084.363	3365.030	Bonded–OH groups
3000–2800	– –	2923.645 –	CH stretching
2400–2000	2103.569 2081.763	2371.581 2292.335	N=C=S stretching C (triple bond) N stretching
	–	2113.989	C (triple bond) C stretching
2000–1650	1992.685 1893.477 –	1991.357 1922.032	CH bending CH bending
1600–1300	1594.726 1541.982	1595.550 –	 N–O stretching
1400–700	1404.934 1375.439 1237.011 1028.248 – 791.064	– 1398.725 1234.126 1149.981 1069.283	O–H bending O–H bending C–O stretching C–N stretching S=O stretching C=C bending

2.6. Equilibrium isotherms

Isotherms that depict the amount of solute that is adsorbed in relation to the unit weight of the sorbent are known as adsorption isotherms. Sometimes, adsorption isotherms are also referred to as equilibrium isotherms. These particular isotherms make use of the equilibrium sorbent concentration at the specified temperature. An adsorption isotherm is a special design that is developed to provide the right experimental data correlation. This design is developed to remove effluents from the system (Sarojini et al., 2021a). Adsorption was performed using both linear and nonlinear adsorption models, with initial concentrations ranging from 0 to 1.5 mg/L.

The several adsorption isotherms listed in Table 1are used to analyze the adsorption capacity.

2.7. Thermodynamic investigations

Investigations of the thermodynamics involved in the adsorption process are also a significant parameter. The adsorption experiment was carried out under a variety of temperature circumstances with the purpose of conducting thermodynamic research. The parameters enthalpy (H), entropy (S), and Gibbs free energy were among those that were calculated (Batool et al., 2018).

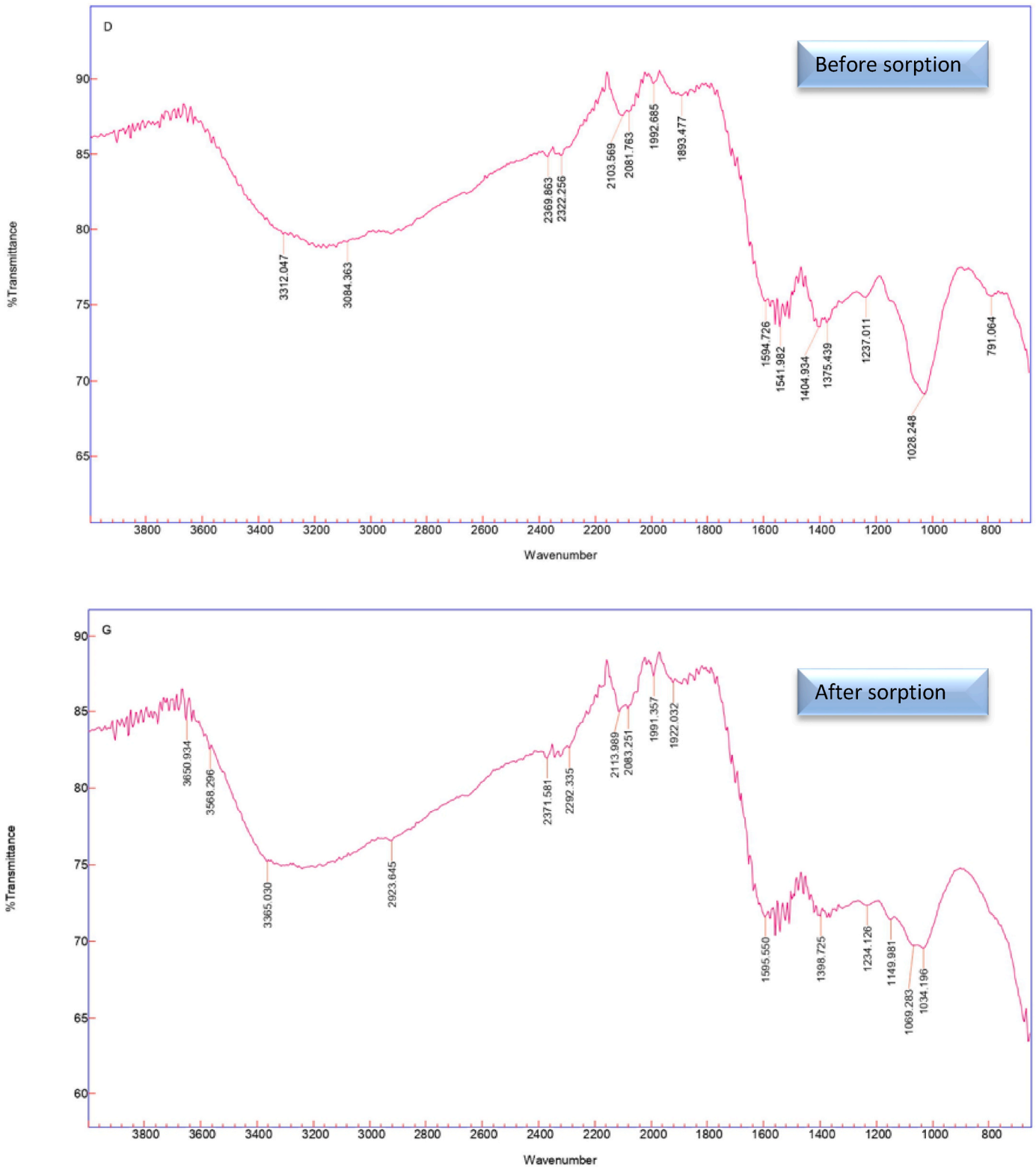


Fig. 4. FTIR Spectra of synthesized Nanocomposite before and after sorption.

$$\Delta G = RT \ln K \quad (3)$$

$$\Delta G = \Delta H - T\Delta S \quad (4)$$

$$K = \frac{q_e}{C_e} \quad (5)$$

3. Result and discussion

BBD was used to explore the dynamic impact that the variables had on the pollutant removal efficiency exhibited by the composite of TiO_2/Fe_2O_3/chitosan. Variables used were depicted in Table 2. Table 3 contains the findings of the biosorption experiment as well as the values that were anticipated by the model equation.

Table 6
Thermodynamic Characteristics for Ibuprofen removal.

Temp(K)	ΔG^o (kJ/mol)	ΔS^o (kJ/mol K)	ΔH^o (kJ/mol)
298.15	−5.4752	0.233	76.23
303.15	−6.5361		
308.15	−4.7275		
313.15	−3.1893		
318.15	−1.6212		
323.15	−0.5468		

The quadratic model for the elimination of ibuprofen is presented as follows in the equations:

$$Y = 89.35 + 10.87\,A + 0.76\,B + 1.97\,C + 0.18\,AB - 0.56\,AC + 0.51\,BC - 33.5\,A^2 + 0.041\,B^2 + 0.41\,C^2 \quad (6)$$

Where Y is the % removal of ibuprofen.

Table 4 displays the results of the ANOVA about the elimination of ibuprofen. It can be seen from the value of the model's F statistic, the high ($R^2 > 0.95$), and the low value of the model's coefficient of variation that the BBD model fits the experimental data very well. The "Pred R^2" and the "Adj R^2" are in persuasive agreement with one another. A suitable signal is specified by the "Adeq Precision-AP" signal-to-noise ratio.

3.1. Effect of variables on sorption of ibuprofen

Three-dimensional graphs were used to illustrate the interactive impacts of various parameters on the elimination of ibuprofen. The dynamic relationship between pH and sorbent concentration is depicted in Fig. 1a. The pH is varied from 5 to 9 and it is inferred that acidic conditions did not promote the removal efficiency of ibuprofen. A maximum ibuprofen removal of 95.2% was achieved when pH was at 7.3 and this value was maintained for other additional experiments. Because the hydrogen ions were deprotonated at a higher pH, the amount of pollutant that could be removed was noticeably increased. The result obtained is well supported by Martinez et al. (2020). They achieved the maximum ibuprofen removal at a pH of 7 using magnetic core-modified silver nanoparticles. They suggest that the dependence of adsorption on pH is associated with the point of zero charge of the adsorbent and the pKa of the ibuprofen. This is due to the Ibuprofen exists as neutral and anionic species when pH is equal to pKa.

The effect of biosorbent mass on the elimination of ibuprofen is investigated by adding biosorbent at concentrations ranging from 0.01 to 0.09 g/L, and it is depicted in Fig. 1a and c. Ibuprofen removal was found to be maximum at a biosorbent concentration of 0.05 g/L. The amount of ibuprofen that was eliminated changed in a way that was directly proportional to the dose of biomass. The presence of a substantial amount of sorption sites that are exposed for the ibuprofen is primarily responsible for the rise in the removal of ibuprofen that was seen when the biosorbent mass was utilized (Jayakumar et al., 2019). As a result, 0.05 g/L was determined to be the optimal mass of biosorbent,

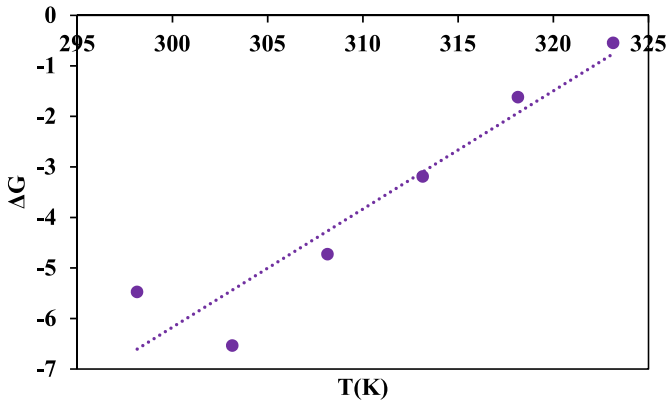


Fig. 6. Thermodynamic plot for Ibuprofen sorption.

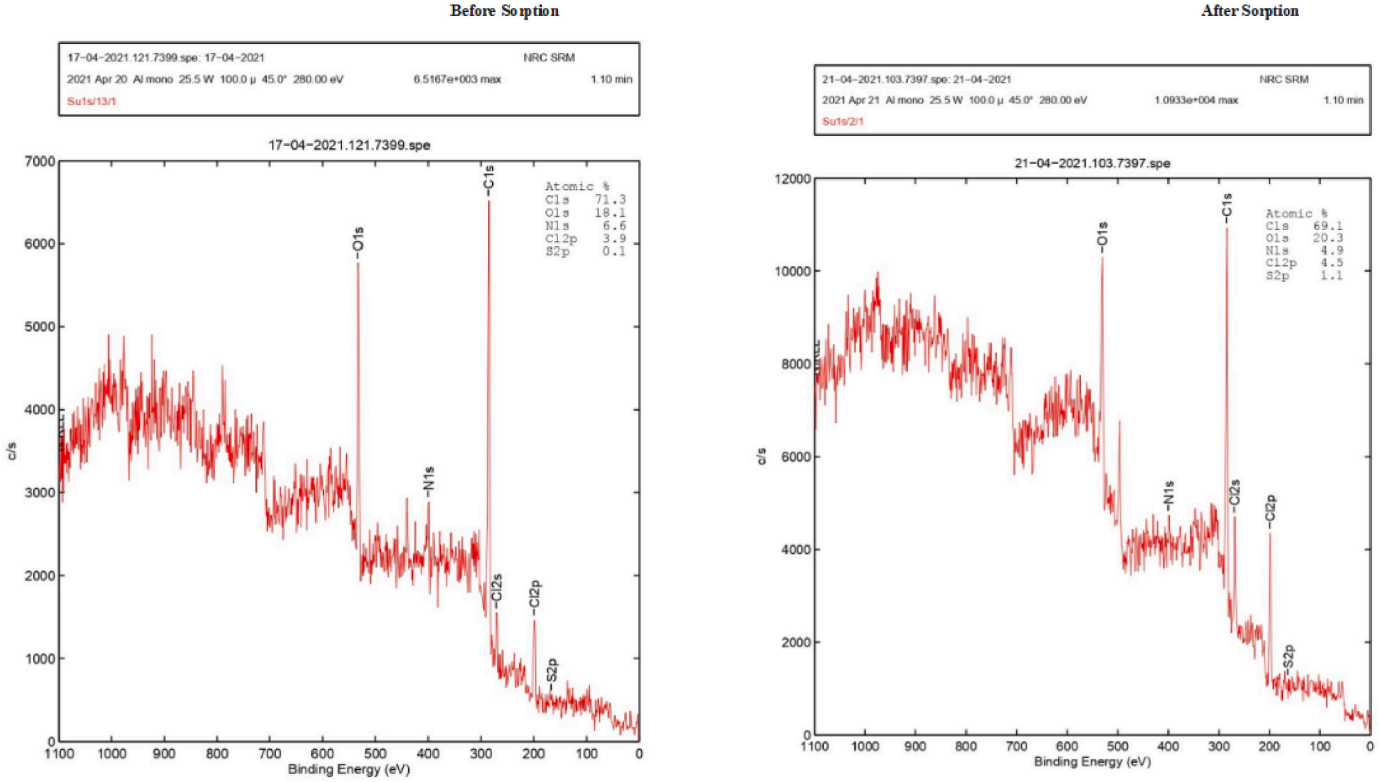


Fig. 5. Xps spectra of nanocomposite before and after sorption.

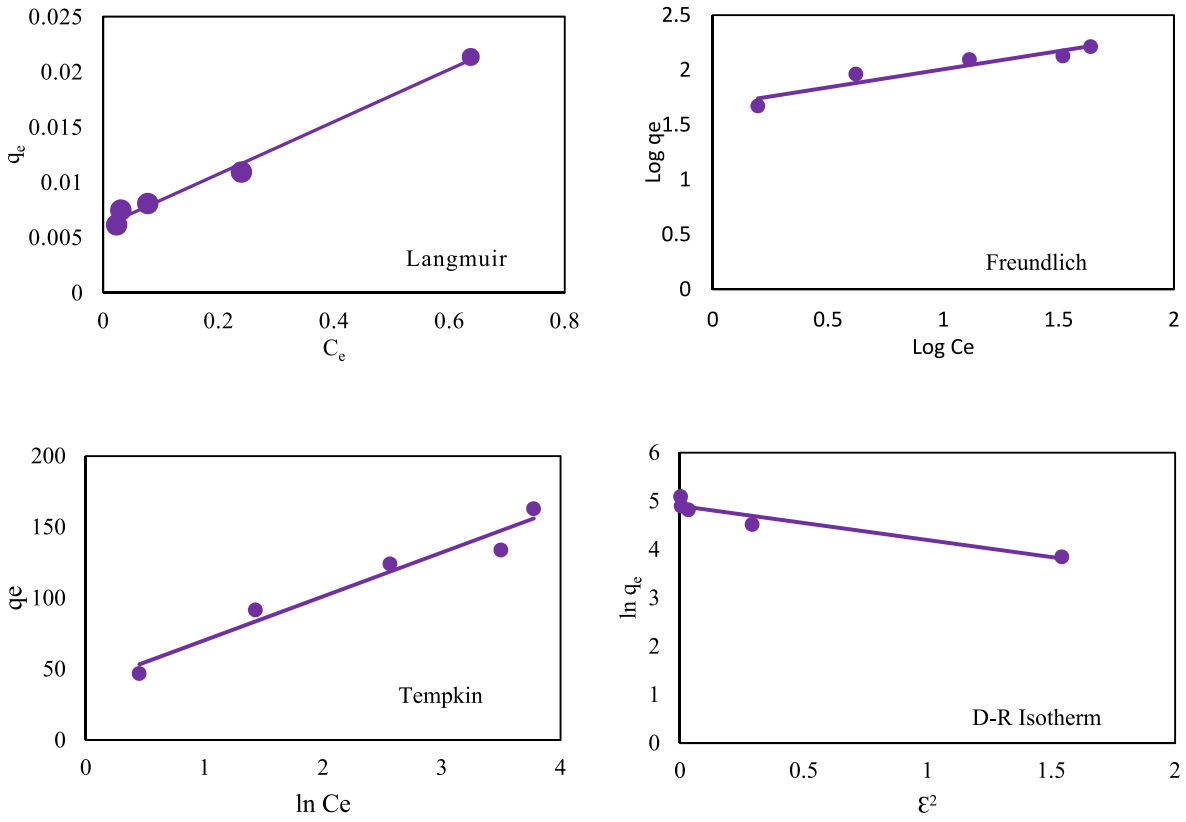


Fig. 7. Isotherm Plots for removal of Ibuprofen.

Table 7
Isotherm Parameters on sorption of ibuprofen.

Isotherm	Linear Parameters	
Langmuir	q_{max}	166.667
	B	0.253
	R^2	0.9906
Freundlich	K_f	47.43
	N	3.02
	R^2	0.9073
D-R	q_{max}	134.262
	B	0.7044
	E	0.842
	R^2	0.9225
Temkin	**B**	30.92
	K_T	3.5747
	R^2	0.9531

Table 8
Ibuprofen sorption kinetic parameters.

Kinetic Model	Parameters for Ibuprofen	
Pseudo First Order	K_1 (min^{-1})	0.03109
	$_R2$	0.9023
Pseudo Second Order	K_2 (g/mg min)	0.000072
	$_R2$	0.53
Intra Particle Diffusion	K_{id} (mg/g $min^{0.5}$)	10.542
	$_R2$	0.8787

and subsequent experimental runs were conducted with this concentration. This is well supported by the literatures (; Sarojini et al., 2021b, 2022) (Jayakumar et al., 2019, 2021).

From 100 to 200 revolutions per minute, the effect of shaking speed is investigated and it is depicted in Fig. 1 b and c. It has been observed that the rate of rotation that produces the greatest amount of ibuprofen removal is 200 rpm. The decreased performance at lower speeds is owing to the fact that the biomass settles at the bottom at a very low shaking speed, which results in a drop in the number of active sites accessible for sorption. This is what causes the reduction in performance seen at lower speeds. Because of the desorption potential of the biosorbent, the removal of ibuprofen becomes less effective as the shaking speed increases (Huang et al., 2017; Jayakumar et al., 2019, 2021). The combinations of pH 7.3, biosorbent mass 0.05 g/L, and agitation speed 200 rpm were shown to be optimal for the maximal removal of ibuprofen using a TiO_2/Fe_2O_3/Chitosan composite.

3.2. Characterization of synthesized nanocomposite

Characterization of sorbent was performed using SEM, XRD, FTIR and XPS and the results obtained are discussed.

3.2.1. SEM analysis

Before and after sorption, the bio sorbent's surface was investigated for changes. The bio sorbent surface seemed hard and rough in the SEM imaging, as shown in Fig. 2 a. After the pollutants were attached, the surface pattern changed and was seen to be enlarged and deformed and as shown in Fig. 2b.

3.2.2. XRD analysis

XRD analysis was utilized for the purpose of determining the phase and crystalline nature of the prepared samples. The XRD spectra of the synthesized TiO_2/Fe_2O_3/Chitosan sample before and after sorption are displayed in Fig. 3. The crystalline nature of the processed sample can be deduced from the strong peaks that were seen in the XRD spectra. A technique called X-ray powder diffraction was used to confirm that there were insufficient distinct diffraction peaks across the pattern, which demonstrated the amorphous nature of the nanocomposites that were created. The existence of chitosan, titanium dioxide, and iron oxide nanoparticles was demonstrated by the primary diffraction peaks of 2Θ

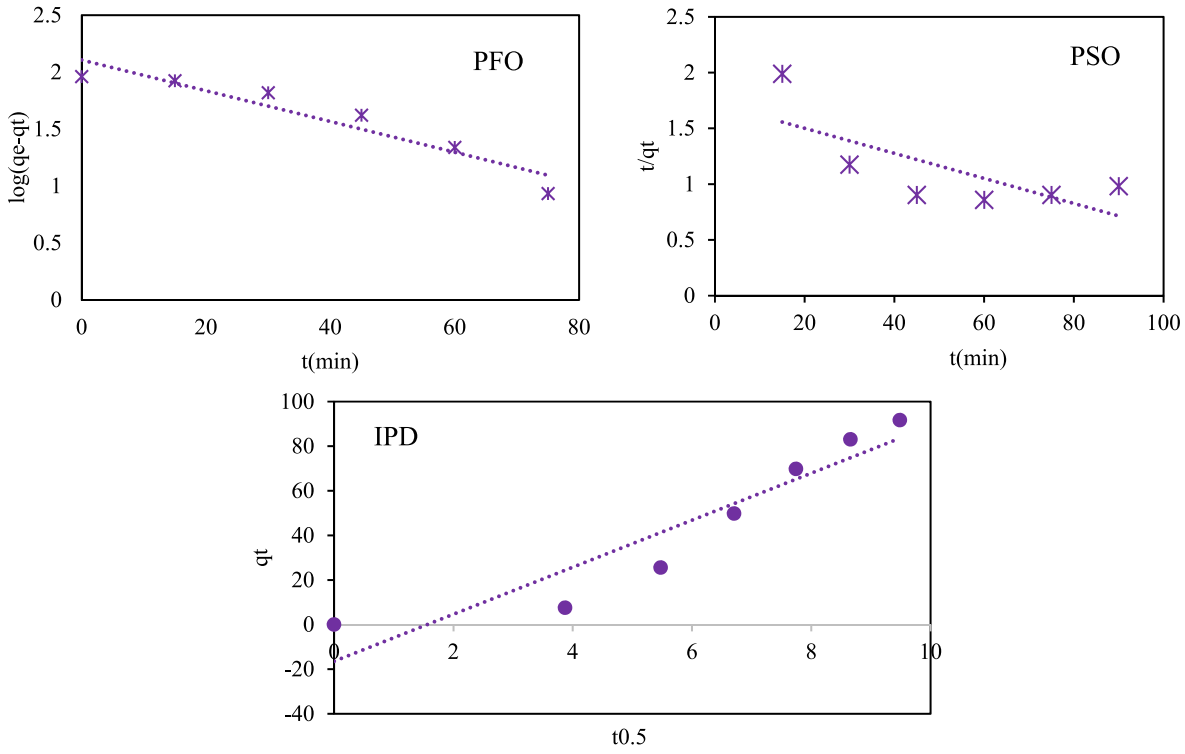


Fig. 8. Kinetic plots for PFO, PSO and IPD

Table 9
Binding affinity of the docked compounds.

Compound	Docking score (kcal/mol)
TiO_2 with ibuprofen	−4.32
Fe_2O_3 with ibuprofen	−5.02
Chitosan with ibuprofen	−5.975

at 18, 30and 48. There were no distinct peaks that could be seen (Rajamehala et al., 2022).

Fig. 3 displays the XRD spectrum TiO_2–Fe_2O_3-chitosan after the adsorption. XRD spectrum of pure TiO_2–Fe_2O_3-chitosan composite shows the presence of plenty of peaks signifying the amorphous nature. After adsorption of ibuprofen, change in XRD was visualized. After adsorption, the amorphous phase gets converted into cystalline form. The presence of distinguished peaks confirms the adsorption of ibuprofen. Formation of new crystals suggests chemisorption has occurred which accounts for change in diffraction pattern.

3.2.3. FTIR analysis

The FTIR provides knowledge on the functional groups present in the surface of sorbent (Belskaya, 2012). Table 5 contains the FTIR spectra of sorbent obtained in the wavenumber range 4000–450 cm^{-1} and the primary functional groups found in sorbent. A broad band arises between 3000 and 3700 cm^{-1} due to the –OH stretching vibration of hydroxyl functional groups, which includes hydrogen bonding, as the broad band of the –OH group in this region indicates the presence of hydrogen bonding in the molecule (Fig. 4). This peak is seen in both untreated and treated sorbents. For all sorbents, the stretching band of –CH appears in the 2900–3000 cm^1 wavenumber range. The peak at 1922 cm^{-1} is attributed to CH bending, and the peak at 1237 cm^{-1} to the C–O functional group. In certain instances, –CN also appears at the 1028 cm^1 and 1149 cm^{-1} values. To attach sorbate to a surface for adsorption purposes, the –OH group and heteroatoms play a crucial role (see Table 6).

3.2.4. XPS analysis

Fig. 5 displays the XPS spectrum TiO_2–Fe_2O_3-chitosan before and after adsorption. Presence of six major peaks at 300, 400, 540, 290, 200 and 170 eV accounts for C 1s, N 1s, O 1s, Cl 2_S Cl 2p and S 2p which was present in the sample. The presence of same elements was observed in spectrum of after adsorption. The variation in the peaks of C 1s, N 1s and O 1s proves that elements are present in the sample and also responsible for adsorption. The change in binding energy of C 1s recommends the contribution of carbon in adsorption of ibuprofen. The change in binding of N 1s suggests the involvement of nitrogen in form of active functional groups amines, imines and positively charged nitrogen atoms in adsorption of ibuprofen. The variation in peak at binding energy of 540 eV accounting to O 1s discloses the fact the increase in oxygen was due to adsorption of ibuprofen ($C_{13}H_{18}O_2$).

3.3. Thermodynamic studies on sorption of ibuprofen

Fig. 6 depicts the influence of temperature on ibuprofen elimination between 298.15 K and 323 K. Because of a boost in particle movement, sorption capacity improves with temperature rise and reaches its maximum at 303.15 K. Variations in temperature have very little impact on the efficiency of the sorption. At a temperature of 323.15 K, ibuprofen elimination was reduced. It implies that greater temperatures are incompatible with ibuprofen adsorption using the nanocomposites developed, and that the reaction is exothermic (see Fig. 7).

The intercept and slope of the plot ΔG vs ΔT for ibuprofen removal using TiO2/Fe2O3/Chitosan nanocomposite are used to calculate the values of ΔH and ΔS, which are displayed in Table .5. (Jayakumar et al., 2021). The positive value of ΔH suggests endothermic sorption, while the positive value of ΔS indicates a rise in randomness at the solid-solution interface during the sorption process. ΔG with a negative value implies spontaneous sorption, while ΔG with a positive value indicates favorable sorption (Mohammed et al., 2018).

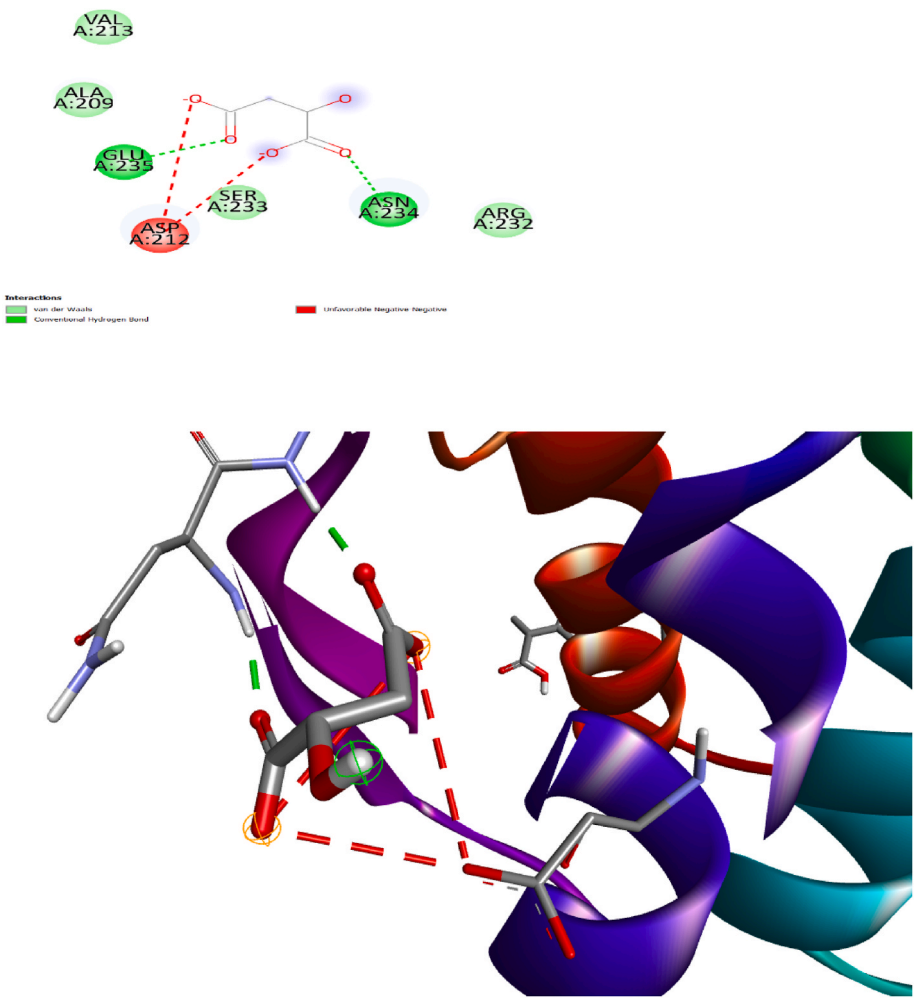


Fig. 9. 2D image showing Chitosan-Ibuprofen Interaction.

3.4. Isotherm studies

The experimental results have been analyzed using linear models of the Langmuir, Freundlich, D-R, and Temkin isotherms, and Table 7 has a listing of the parameters that correspond to these models.

The Langmuir isotherm is dependent on the regularity and homogeneity of the sorbent, and it must adhere to a surface that has a significant number of empty sites to be single-layer sorption. The assumption that the energies of all adsorbents are the same is the model's most significant shortcoming.

The R_L defines the favorability of the isotherm, which must be less than one for fitness.

$$R_{L=\frac{1}{1+(1+bC_o)}} \tag{7}$$

where C_o - initial concentration of ibuprofen.

A correlation coefficient of greater than 0.90 indicates the compatibility of experimental data with model prediction. It is observed that linear ($R^2 = 0.9906$) model of the Langmuir isotherm exhibit strong correlation. The results demonstrate that the correctness of the aforementioned isothermal model reflects a homogeneous adsorption process. The constant value of the Freundlich isotherm between 0 and 1 implies good adsorption. Here, (1/n) = 0.3311 indicates that ibuprofen sorption was favorable.

Accordingly, the Langmuir adsorption isotherm is advantageous for experimental results on the sorption of ibuprofen on TiO_2/Fe_2O_3/Chitosan nanocomposite.

The strong R^2 value of the Temkin isotherm suggests that the model fits the data well. In the D-R isotherm, physical adsorption occurs when E is less than 8 kJ/mol, while chemical adsorption occurs only when E is larger than 8 kJ/mol (Sarojini et al., 2021a). E = 0.842, as shown in the table, showing that the process was physical. On the basis of the observations, one can conclude that the sorption mechanisms tend to adhere to the Langmuir model.

3.5. Kinetic studies

Since kinetics enables us to comprehend the adsorption process and potential rate-limiting phases, it is necessary for comprehending the effects of pollutant removal on sorbent to have a concept of kinetics. Also, it is vital to have an understanding of the kinetics of pollutant adsorption to determine the ideal settings for the method that involves the large-scale batch removal of pollutants. To explore the rate of ibuprofen adsorption on TiO_2/Fe_2O_3/Chitosan Nanocomposite, a variety of kinetic models have been utilized.

A pseudo-first-order equation was presented by Lagergren (Ho, 2004)

$$\log(q_e - q_t) = \log q_e - \frac{K_1}{2.303}t \tag{8}$$

The pseudo second order model predicts the behavior of sorption during the entire adsorption time (Ho and McKay, 1999)

$$\frac{t}{q_t} = \frac{1}{K_2 q_e^2} + \frac{1}{q_e}t \tag{9}$$

(Kamaraj et al., 2018, 2016; Kamaraj and Vasudevan, 2016; Moradi et al., 2018).

Diffusion research was carried out to better understand the transport processes connected with the adsorption of liquid particles onto a solid substrate (Weber and Morris, 1963). The resulting equation is as follows:

$$q_t = K_{id} t^{0.5} + C \quad (10)$$

Table 8 displays the values of the kinetic model's parameters, and Fig. 8 depicts their charts. Based on the Intra particle diffusion investigation, a strong correlation coefficient was discovered. R^2 values indicates that the pseudo first order model is outperforms compared to the pseudo second order model.

3.6. Docking studies

For docking investigations of protein-ligand binding, we use the AutoDock tool (http://autodock.scripps.edu/resources/references). After preparing the protein-ligand molecules, they were saved in PDBQT format (. Pdbqt file extension). It was decided to form the grid box. The Genetic Algorithm (GA) was carried out with a total of fifty iterations, and the results were saved in Grid Parameter File (. Dpf format). After that, the Grid Log File [GLG] and Dock Log File [DLG] executive tools were started up to generate Grid Log File [GLG] and Dock Log File [DLG] files. The result was examined, and its position in the ranking was determined, based on the binding affinity score of the macromolecule drug interaction. In preparation for further investigation, the protein-ligand complex that comprises the complicated molecule was stored in pdbqt format. Discovery studio from BIOVIA is utilized to investigate and visualize the 2D structures, as well as the interactions between proteins and ligands.

Fe_2O_3, TiO_2, and Chitosan compounds were docked with ligand ibuprofen. Chitosan-ligand binding showed a better result when compared to Fe_2O_3 and TiO_2. The complex Chitosan with ibuprofen showed the best affinity of −6.529. The 2D diagram showed the interaction between the Chitosan – ibuprofen complex. Table 9 shows the binding affinity of the docked compounds and depicted in Fig. 9.

4. Conclusion

In this research work, the successful synthesis of the Metal-Metal-Polymer nanocomposite was explored along with its application for ibuprofen removal. Characterization of the surface properties of the composite before and after elimination of ibuprofen is also performed to confirm the sorption. Through the use of the BBD technique, the optimum conditions (pH - 7.3, biosorbent mass - 0.05 g/L, and agitation speed - 200 rpm) are found for the maximum removal of ibuprofen. The highest elimination of ibuprofen was found to be 95.2% under the optimized conditions. The kinetics of ibuprofen sorption by TiO_2/Fe_2O_3/Chitosan Nanocomposite was represented by PFO with high R^2 value of 0.9023. The adsorption was determined to be monolayer, spontaneous, and endothermic using isotherms and thermodynamics studies. As the temperature rose, there was a corresponding rise in the amount of pollutant that could be removed effectively. The examination by the SEM demonstrated that the surface structure was beneficial, leading to improved sorption of ibuprofen. The results of this study suggest that, the TiO_2/Fe_2O_3/Chitosan Nanocomposite is a promising material for the sorption of ibuprofen from diverse water-based media.

Credit author statement

M.Rajamehala - Conceptualization, Data curation, Investigation, Validation, Software, Visualization, Writing – original draft, **A.Muthu kumara pandian** – Resources, Formal analysis, Software, Supervision, Writing – review & editing, **M.Rajasimman** - Resources, Methodology, Writing – review & editing, **B.Gopalakrishnan** - Methodology, Supervision, Validation, Writing – review & editing

Declaration of competing interest

The authors declare that they have no known competing financial interests or personal relationships that could have appeared to influence the work reported in this paper.

Data availability

The authors do not have permission to share data.

References

Aguilar-Pérez, K.M., Avilés-Castrillo, J.I., Ruiz-Pulido, G., Medina, D.I., Parra-Saldivar, R., Iqbal, H.M.N., 2021. Nanoadsorbents in focus for the remediation of environmentally-related contaminants with rising toxicity concerns. Sci. Total Environ. 779 https://doi.org/10.1016/j.scitotenv.2021.146465.

Ahmad, N., Sultana, S., Khan, M.Z., Sabir, S., 2020. Chitosan based nanocomposites as efficient adsorbents for water treatment. Mod. Age Waste Water Probl. 69–83. https://doi.org/10.1007/978-3-030-08283-3_4.

Ahmed, M.J., 2017. Adsorption of non-steroidal anti-inflammatory drugs from aqueous solution using activated carbons: Review. J. Environ. Manag. 190, 274–282. https://doi.org/10.1016/j.jenvman.2016.12.073.

Ali, I., Al-Othman, Z.A., Alwarthan, A., 2016. Synthesis of composite iron nano adsorbent and removal of ibuprofen drug residue from water. J. Mol. Liq. 219, 858–864. https://doi.org/10.1016/j.molliq.2016.04.031.

Balaji, S., Guda, R., Mandal, B., Kasula, M., Ubba, E., Nawaz Khan, F.R., 2019. Green synthesis of nano-titania (TiO2 NPs) utilizing aqueous Eucalyptus globulus leaf extract: applications in the synthesis of 4H-pyran derivatives. Res. Chem. Intermed. 1–13. https://doi.org/10.1007/s11164-018-03720-0.

Batool, F., Akbar, J., Iqbal, S., Noreen, S., Bukhari, S.N.A., 2018. Study of isothermal, kinetic, and thermodynamic parameters for adsorption of cadmium: an overview of linear and nonlinear approach and error analysis. Bioinorgan. Chem. Appl., 3463724 https://doi.org/10.1155/2018/3463724, 2018.

Belskaya, O.B., 2012. In: Danilova, I.G. (Ed.), FTIR Spectroscopy of Adsorbed Probe Molecules for Analyzing the Surface Properties of Supported Pt (Pd) Catalysts. IntechOpen, Rijeka. https://doi.org/10.5772/36275. Ch. 7.

Bhanvase, B.A., Veer, A., Shirsath, S.R., Sonawane, S.H., 2019. Ultrasound assisted preparation, characterization and adsorption study of ternary chitosan-ZnO-TiO2 nanocomposite: advantage over conventional method. Ultrason. Sonochem. 52, 120–130. https://doi.org/10.1016/j.ultsonch.2018.11.003.

Bhuiyan, M.S.H., Miah, M.Y., Paul, S.C., AkaT, Das, Saha, O., Rahaman, M.M., Sharif, M. J.I., Habiba, O., Ashaduzzaman, M., 2020. Green synthesis of iron oxide nanoparticle using Carica papaya leaf extract: application for photocatalytic degradation of remazol yellow RR dye and antibacterial activity. Heliyon 6, e04603. https://doi.org/10.1016/j.heliyon.2020.e04603.

Chakraborty, P., Singh, S., Gorai, I., Singh, D., Rahman, W., Halder, G., 2020. Explication of physically and chemically treated date stone biochar for sorptive remotion of ibuprofen from aqueous solution. J. Water Proc. Eng. 33, 101022 https://doi.org/10.1016/j.jwpe.2019.101022.

Dragoi, E.-N., Vasseghian, Y., 2021. Modeling of mass transfer in vacuum membrane distillation process for radioactive wastewater treatment using artificial neural networks. Toxin Rev. 40, 1526–1535. https://doi.org/10.1080/15569543.2020.1744659.

Dubinin, M.M., 1960. The potential theory of adsorption of gases and vapors for adsorbents with energetically nonuniform surfaces. Chem. Rev. 60, 235–241. https://doi.org/10.1021/cr60204a006.

Freundlich, H.M.F., 1906. Over the adsorption in solution. J. Phys. Chem. 57, 385–471.

Fröhlich, A.C., Foletto, E.L., Dotto, G.L., 2019. Preparation and characterization of NiFe2O4/activated carbon composite as potential magnetic adsorbent for removal of ibuprofen and ketoprofen pharmaceuticals from aqueous solutions. J. Clean. Prod. 229, 828–837. https://doi.org/10.1016/j.jclepro.2019.05.037.

Gilevska, T., Gehre, M., Richnow, H., 2015. Multidimensional isotope analysis of carbon, hydrogen and oxygen as tool for identification of the origin of ibuprofen. J. Pharm. Biomed. Anal. 115, 410–417. https://doi.org/10.1016/j.jpba.2015.07.030.

Heberer, T., 2002. Occurrence, fate, and removal of pharmaceutical residues in the aquatic environment: a review of recent research data. Toxicol. Lett. 131, 5–17. https://doi.org/10.1016/s0378-4274(02)00041-3.

Ho, Y.-S., 2004. Citation review of lagergreen kinetic rate equation on adsorption reaction. Scientometrics 59, 171–177. https://doi.org/10.1023/B:SCIE.0000013305.99473.cf.

Ho, Y.S., McKay, G., 1999. Pseudo-second order model for sorption processes. Process Biochem. (Oxford, U. K.) 34, 451–465. https://doi.org/10.1016/S0032-9592(98)00112-5.

Jayakumar, R., Rajasimman, M., Karthikeyan, C., 2019. Column studies on sorption of Cr (VI) from aqueous and electroplating wastewater using acid-treated marine brown algae Sargassum myriocystum. ENERGY SOURCES PART A-RECOVERY Util. Environ. Eff.

Huang, Z., Li, Y., Chen, W., Shi, J., Zhang, N., Wang, X., Li, Z., Gao, L., Zhang, Y., 2017. Modified bentonite adsorption of organic pollutants of dye wastewater. Mater. Chem. Phys. 202, 266–276. https://doi.org/10.1016/j.matchemphys.2017.09.028.

Jayakumar, V., Govindaradjane, S., Rajasimman, M., 2021. Efficient adsorptive removal of zinc by green marine macro alga caulerpa scalpelliformis –characterization, optimization, modeling, isotherm, kinetic, thermodynamic, desorption and regeneration studies. Surface. Interfac. 22, 100798 https://doi.org/10.1016/j.surfin.2020.100798.

Kamal, A., Cincinelli, A., Martellini, T., Malik, R.N., 2015. A review of PAH exposure from the combustion of biomass fuel and their less surveyed effect on the blood parameters. Environ. Sci. Pollut. Res. 22, 4076–4098. https://doi.org/10.1007/s11356-014-3748-0.

Kamaraj, R., Pandiarajan, A., Jayakiruba, S., Naushad, M., Vasudevan, S., 2016. Kinetics, thermodynamics and isotherm modeling for removal of nitrate from liquids by facile one-pot electrosynthesized nano zinc hydroxide. J. Mol. Liq. 215, 204–211. https://doi.org/10.1016/j.molliq.2015.12.032.

Kamaraj, R., Pandiarajan, A., Vasudevan, Sudharshan, Vasudevan, Subramanyan, 2018. Facile one-pot electrosynthesis of zinc hydroxide for the adsorption of hazardous 2-(2-methyl-4-chlorophenoxy) propionic acid (MCPP) from water and its modelling studies. J. Environ. Chem. Eng. 6, 2017–2026. https://doi.org/10.1016/j.jece.2018.03.011.

Kamaraj, R., Vasudevan, S., 2016. Facile one-pot electrosynthesis of Al(OH)3 – kinetics and equilibrium modeling for adsorption of 2,4,5-trichlorophenoxyacetic acid from aqueous solution. New J. Chem. 40, 2249–2258. https://doi.org/10.1039/C5NJ02407B.

Langmuir, I., 1916. The constitution and fundamental properties of solids and liquids. Part I. Solids. J. Am. Chem. Soc. 38, 2221–2295. https://doi.org/10.1021/ja02268a002.

Leong, S., Razmjou, A., Wang, K., Hapgood, K., Zhang, X., Wang, H., 2014. TiO2 based photocatalytic membranes: a review. J. Membr. Sci. 472, 167–184. https://doi.org/10.1016/j.memsci.2014.08.016.

Liu, Y., Yuan, Y., Ramya, G., Mohan Singh, S., Thuy Lan Chi, N., Pugazhendhi, A., Xia, C., Mathimani, T., 2022. A review on the promising fuel of the future – biobutanol; the hindrances and future perspectives. Fuel 327, 125166. https://doi.org/10.1016/j.fuel.2022.125166.

Mahmoudi, B.M., Simchi, A., Vali, H., Imani, M., 2009. Cytotoxicity and cell cycle effects of bare and poly (vinyl alcohol)-coated iron oxide nanoparticles in mouse fibroblasts. https://doi.org/10.1002/adbi.200900004, 243, 250.

Mitra, S., Sarkar, A., Sen, S., 2017. Removal of chromium from industrial effluents using nanotechnology: a review. Nanotechnol. Environ. Eng. 2, 11. https://doi.org/10.1007/s41204-017-0022-y.

Mohammed, N.A.S., Abu-Zurayk, R.A., Hamadneh, I., Al-Dujaili, A.H., 2018. Phenol adsorption on biochar prepared from the pine fruit shells: equilibrium, kinetic and thermodynamics studies. J. Environ. Manag. 226, 377–385. https://doi.org/10.1016/j.jenvman.2018.08.033.

Mohmood, I., Lopes, C.B., Lopes, I., Ahmad, I., Duarte, A.C., Pereira, E., 2013. Nanoscale materials and their use in water contaminants removal—a review. Environ. Sci. Pollut. Res. 20, 1239–1260. https://doi.org/10.1007/s11356-012-1415-x.

Nourmoradi, H., Moghadam, K.F., Jafari, A., Kamarehie, B., 2018. Removal of acetaminophen and ibuprofen from aqueous solutions by activated carbon derived from Quercus Brantii (Oak) acorn as a low-cost biosorbent. J. Environ. Chem. Eng. 6, 6807–6815. https://doi.org/10.1016/j.jece.2018.10.047.

Rainsford, K.D., 2012. Ibuprofen: pharmacology, therapeutics and side effects, ibuprofen: pharmacology, therapeutics and side effects. https://doi.org/10.1007/978-3-0348-0496-7.

Rajamehala, M., Pandian, A.M., Rajasimman, M., Gopalakrishnan, B., 2022. Synthesis of metal -based functional nanocomposite material and its application for the elimination of paracetamol from synthetic wastewater. Chemosphere 136530. https://doi.org/10.1016/j.chemosphere.2022.136530.

Rasheed, T., Hassan, A.A., Kausar, F., Sher, F., Bilal, M., Iqbal, H.M.N., 2020. Carbon nanotubes assisted analytical detection – sensing/delivery cues for environmental and biomedical monitoring. TrAC Trends Anal. Chem. (Reference Ed.) 132, 116066. https://doi.org/10.1016/j.trac.2020.116066.

Rasheed, T., Nabeel, F., Adeel, M., Rizwan, K., Bilal, M., Iqbal, M.N., 2019. Carbon nanotubes-based cues : a pathway to future sensing and detection of hazardous pollutants, 292. https://doi.org/10.1016/j.molliq.2019.111425.

Sarojini, G., Venkatesh Babu, S., Rajamohan, N., Rajasimman, M., 2022. Performance evaluation of polymer-marine biomass based bionanocomposite for the adsorptive removal of malachite green from synthetic wastewater. Environ. Res. 204, 112132 https://doi.org/10.1016/j.envres.2021.112132.

Sarojini, G., Venkatesh Babu, S., Rajamohan, N., Senthil Kumar, P., Rajasimman, M., 2021a. Surface modified polymer-magnetic-algae nanocomposite for the removal of chromium- equilibrium and mechanism studies. Environ. Res. 201, 111626 https://doi.org/10.1016/j.envres.2021.111626.

Sarojini, G., Venkateshbabu, S., Rajasimman, M., 2021b. Facile synthesis and characterization of polypyrrole - iron oxide – seaweed (PPy-Fe3O4-SW) nanocomposite and its exploration for adsorptive removal of Pb(II) from heavy metal bearing water. Chemosphere 278, 130400. https://doi.org/10.1016/j.chemosphere.2021.130400.

Show, S., Chakraborty, P., Karmakar, B., Halder, G., 2021. Sorptive and microbial riddance of micro-pollutant ibuprofen from contaminated water: a state of the art review. Sci. Total Environ. 786, 147327 https://doi.org/10.1016/j.scitotenv.2021.147327.

Streit, A.F.M., Collazzo, G.C., Druzian, S.P., Verdi, R.S., Foletto, E.L., Oliveira, L.F.S., Dotto, G.L., 2021. Adsorption of ibuprofen, ketoprofen, and paracetamol onto activated carbon prepared from effluent treatment plant sludge of the beverage industry. Chemosphere 262, 128322. https://doi.org/10.1016/j.chemosphere.2020.128322.

Temkin, M.J., Pyzhev, V., 1940. Kinetics of ammonia synthesis on promoted iron catalysts. Acta Phy. Chem. URSS 12, 217–222.

Thomas, F., 2017. Pharmaceutical waste in the environment: a cultural perspective. Public Heal. Panor. 3, 127–132.

Tiwari, B., Sellamuthu, B., Ouarda, Y., Drogui, P., Tyagi, R.D., Buelna, G., 2017. Review on fate and mechanism of removal of pharmaceutical pollutants from wastewater using biological approach. Bioresour. Technol. 224, 1–12. https://doi.org/10.1016/j.biortech.2016.11.042.

Vasseghian, Y., Arunkumar, P., Joo, S.-W., Gnanasekaran, L., Kamyab, H., Rajendran, S., Balakrishnan, D., Chelliapan, S., Klemeš, J.J., 2022a. Metal-organic framework-enabled pesticides are an emerging tool for sustainable cleaner production and environmental hazard reduction. J. Clean. Prod. 373, 133966 https://doi.org/10.1016/j.jclepro.2022.133966.

Vasseghian, Y., Le, V.T., Joo, S.-W., Dragoi, E.-N., Kamyab, H., Chelliapan, S., Klemeš, J. J., 2022b. Spotlighting graphene-based catalysts for the mitigation of environmentally hazardous pollutants to cleaner production: a review. J. Clean. Prod. 365, 132702 https://doi.org/10.1016/j.jclepro.2022.132702.

Velazquez, A.E., 2020. Sorption, Uptake, Trophic Transfer and Immunotoxicity of Microplastics and Nanoplastics in the Aquatic Environment. Faculty of Texas Tech University.

Weber, W., Morris, J., 1963. Kinetics of adsorption on carbon from solution. J. Sanit. Eng. Div. 89, 31–59.

Wu, Y., Liang, Y., Mei, C., Cai, L., Nadda, A., Le Q, Van, Peng, Y., Lam, S.S., Sonne, C., Xia, C., 2022. Advanced nanocellulose-based gas barrier materials: present status and prospects. Chemosphere 286, 131891. https://doi.org/10.1016/j.chemosphere.2021.131891.

Xia, C., Pathy, A., Paramasivan, B., Ganeshan, P., Dhamodharan, K., Juneja, A., Kumar, D., Brindhadevi, K., Kim, S.-H., Rajendran, K., 2022. Comparative study of pyrolysis and hydrothermal liquefaction of microalgal species: analysis of product yields with reaction temperature. Fuel 311, 121932. https://doi.org/10.1016/j.fuel.2021.121932.

Yasser, V., Elena, N.D., 2018. Modeling and optimization of acid blue 193 removal by UV and peroxydisulfate process. J. Environ. Eng. 144, 6018003 https://doi.org/10.1061/(ASCE)EE.1943-7870.0001405.

Zhang, H., Ju, S., Jin, X., Yuan, Y., Wu, Y., Nadda, A.K., Pugazhendhi, A., Cai, L., Xia, C., 2022. A review of sensor applications towards precise control of pyrolysis of solid waste and biomasses. Renew. Sustain. Energy Rev. 169, 112915 https://doi.org/10.1016/j.rser.2022.112915.